CERES Angular Distribution Model Working Group Report

Wenying Su
Wenying.Su-1@nasa.gov
NASA LaRC, Hampton VA

Joseph Corbett Lusheng Liang
Zachary Eitzen Victor Sothcott
Walter Miller
SSAI, Hampton VA

From radiance to flux: angular distribution models

- Sort observed radiances into angular bins over different scene types;
- Integrate radiance over all θ and ϕ to estimate the anisotropic factor for each scene type;
- Apply anisotropic factor to observed radiance to derive TOA flux;

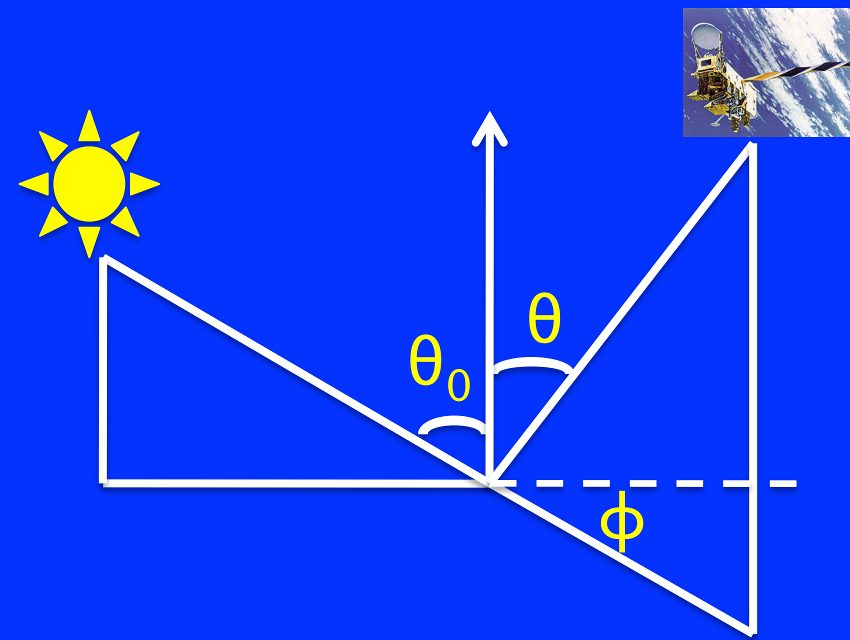

$$R(\theta_0, \theta, \phi) = \frac{\pi \hat{I}(\theta_0, \theta, \phi)}{\int_0^{2\pi} \int_0^{\frac{\pi}{2}} \hat{I}(\theta_0, \theta, \phi) cos\theta sin\theta d\theta d\phi} = \frac{\pi \hat{I}(\theta_0, \theta, \phi)}{\hat{F}(\theta_0)}$$

$$F(\theta_0) = \frac{\pi I_o(\theta_0, \theta, \phi)}{R(\theta_0, \theta, \phi)}$$

Edition 4 ADM methodology and validation papers are published!

- W. Su, J. Corbett, Z. A. Eitzen, and L. Liang. Next-generation angular distribution models for top-of-atmosphere radiative flux calculation from the CERES instruments: Methodology. Atmos. Meas. Tech., 8, 611-632, doi:10.5194/amt-8-611-2015,2015.
- W. Su, J. Corbett, Z. A. Eitzen, and L. Liang. Next-generation angular distribution models for top-of-atmosphere radiative flux calculation from the CERES instruments: Validation. Atmos. Meas. Tech., 8,3297-3313, doi:10.5194/amt-8-3297-2015, 2015.
- J. Corbett and W. Su. Accounting for the effects of sastrugi in the CERES clear-sky Antarctic shortwave angular distribution models. Atmos. Meas. Tech., 8, 3163-3175, doi:10.5194/amt-8-3163-2015, 2015.

Atmos. Meas. Tech., 8, 611–632, 2015
www.atmos-meas-tech.net/8/611/2015/
doi:10.5194/amt-8-611-2015

Atmospheric Measurement Techniques
Open Access

Next-generation angular distribution models for top-of-atmosphere radiative flux calculation from CERES instruments: methodology

W. Su[1], J. Corbett[2], Z. Eitzen[2], and L. Liang[2]
[1]MS420, NASA Langley Research Center, Hampton, Virginia, USA
[2]Science Systems & Applications, Inc., Hampton, Virginia, USA
Correspondence to: W. Su (wenying.su-1@nasa.gov)

Received: 20 June 2014 – Published in Atmos. Meas. Tech. Discuss.: 27 August 2014
Revised: 22 December 2014 – Accepted: 7 January 2015 – Published: 5 February 2015

Atmos. Meas. Tech., 8, 3297–3313, 2015
www.atmos-meas-tech.net/8/3297/2015/
doi:10.5194/amt-8-3297-2015

Atmospheric Measurement Techniques
Open Access

Next-generation angular distribution models for top-of-atmosphere radiative flux calculation from CERES instruments: validation

W. Su[1], J. Corbett[2], Z. Eitzen[2], and L. Liang[2]
[1]MS420, NASA Langley Research Center, Hampton, Virginia, USA
[2]Science Systems & Applications, Inc., Hampton, Virginia, USA
Correspondence to: W. Su (wenying.su-1@nasa.gov)

Received: 8 April 2015 – Published in Atmos. Meas. Tech. Discuss.: 4 May 2015
Revised: 24 July 2015 – Accepted: 29 July 2015 – Published: 14 August 2015

Atmos. Meas. Tech., 8, 3163–3175, 2015
www.atmos-meas-tech.net/8/3163/2015/
doi:10.5194/amt-8-3163-2015

Atmospheric Measurement Techniques
Open Access

Accounting for the effects of sastrugi in the CERES clear-sky Antarctic shortwave angular distribution models

J. Corbett[1] and W. Su[2]
[1]Science Systems and Applications, Inc., NASA Langley Research Center, Mail Stop 420, Hampton, Virginia 23681-2199, USA
[2]NASA Langley Research Center, Mail Stop 420, Hampton, Virginia 23681-2199, USA
Correspondence to: J. Corbett (joseph.g.corbett@nasa.gov)

Received: 20 November 2014 – Published in Atmos. Meas. Tech. Discuss.: 12 January 2015
Revised: 25 June 2015 – Accepted: 23 July 2015 – Published: 10 August 2015

From Aqua to S-NPP

- Footprint size for S-NPP is larger than that for Aqua.
- Cloud properties retrieved from VIIRS can also be different from those retrieved from MODIS.

	Aqua	S-NPP
Launch	May 4, 2002	Oct. 28, 2011
Altitude	705 km	824 km
Inclination	98.14°	98.75°
Period	98.4 min	101.4 min

- How do these differences affect the S-NPP fluxes inverted using Aqua ADMs ?
  - Examine the sigmoidal fits over ocean developed using Aqua and S-NPP data
  - Simulate Aqua and S-NPP observations using MODIS pixel level data
  - Examine MISR anisotropy for different size of footprints

Angular distribution model over cloudy ocean

- For glint angle > 20°:
  - Average instantaneous radiances into 775 intervals of ln(fτ);
  - Apply a five-parameter sigmoidal fit to mean radiance and ln(fτ);

$$I = I_0 + \frac{a}{[1 + e^{-(x-x_0)/b}]^c}$$

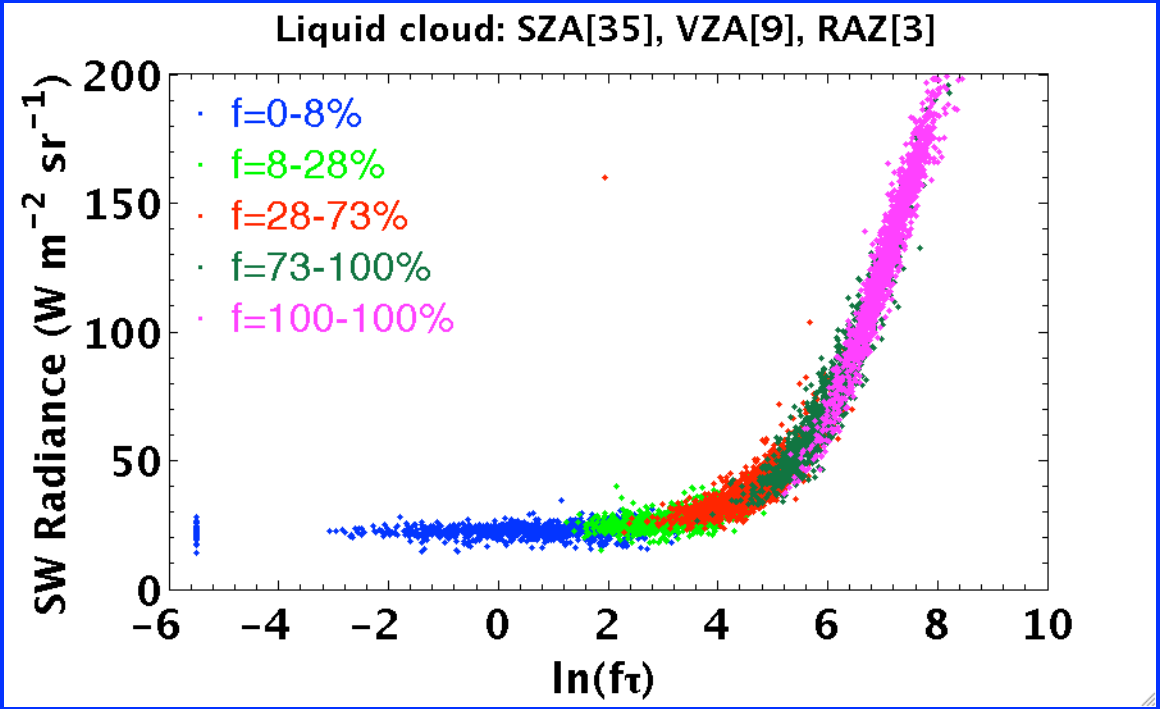

f: cloud fraction
τ: cloud optical depth

Sigmoidal fits from Aqua and S-NPP: using 4 months of data

Liquid clouds Aqua NPP

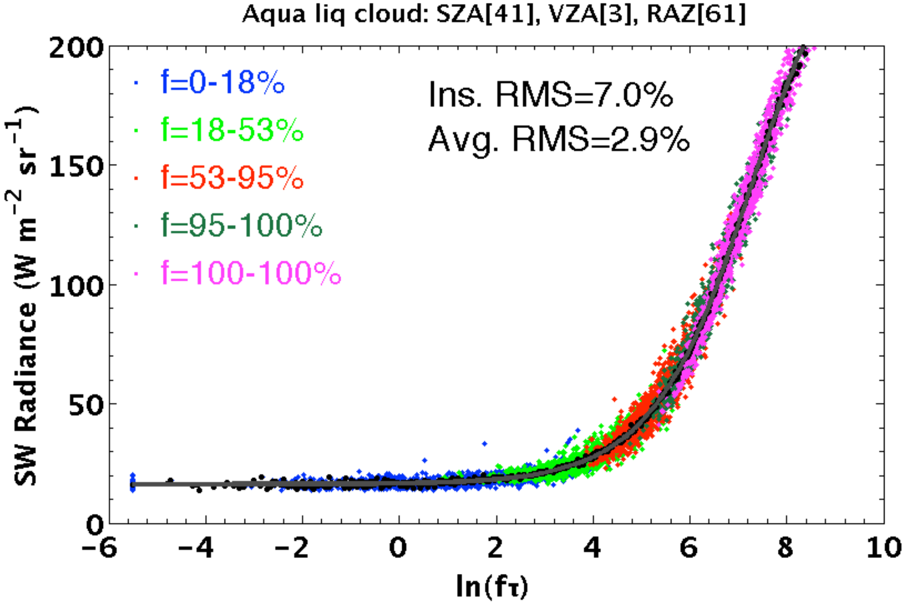

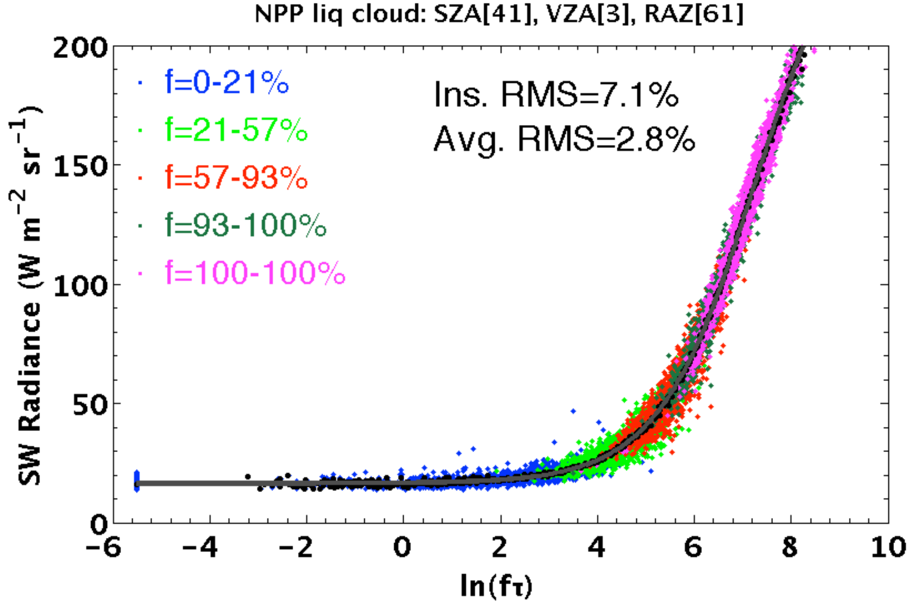

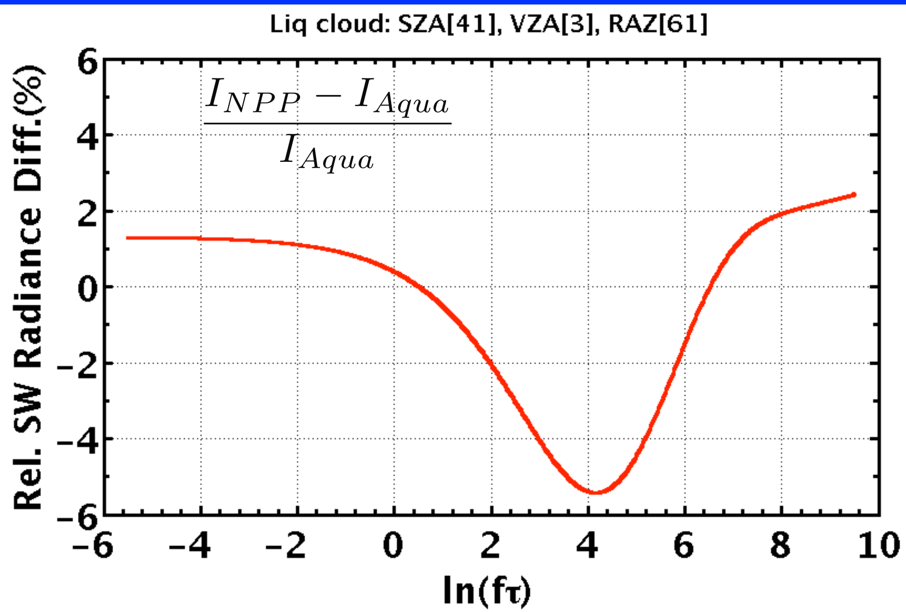

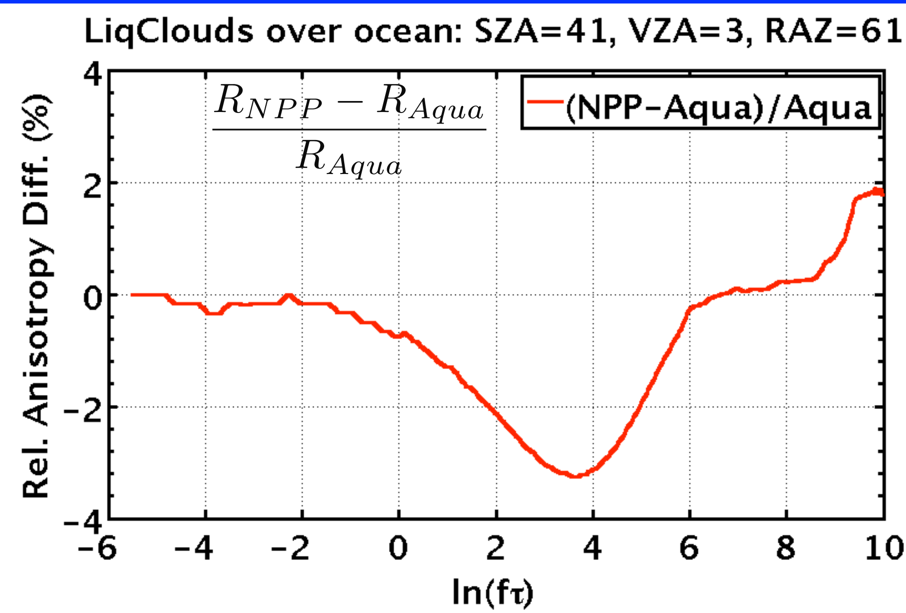

Sigmoidal fits from Aqua and S-NPP: using 4 months of data

Ice clouds Aqua NPP

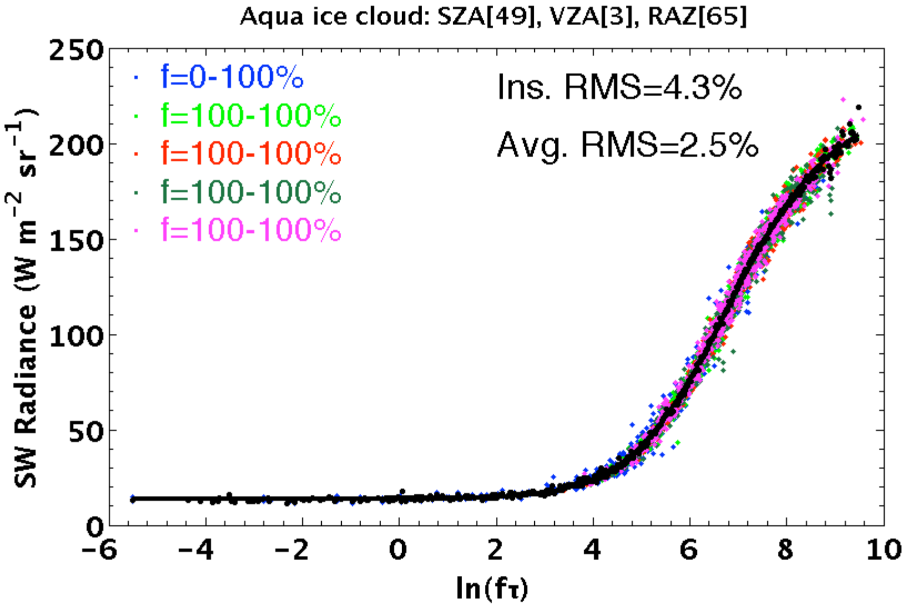

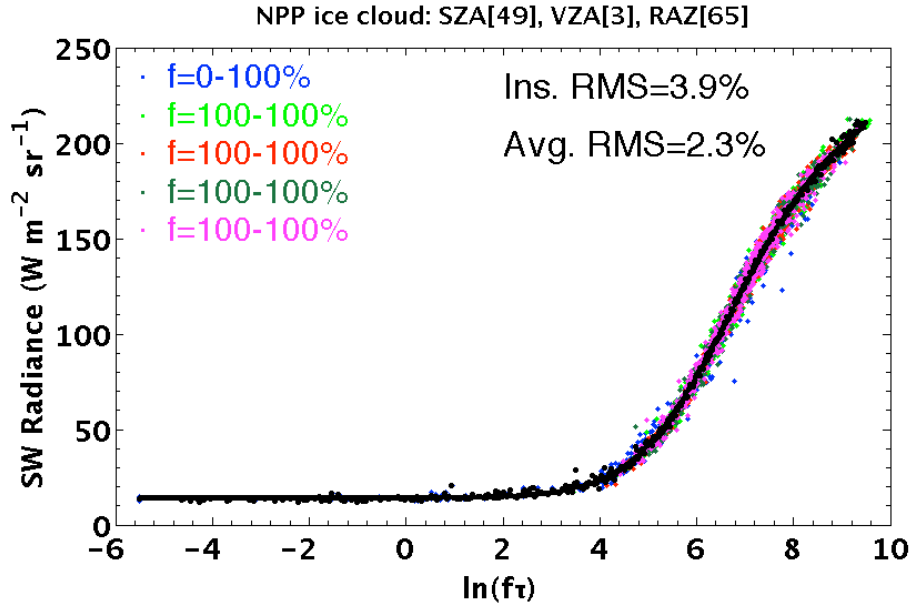

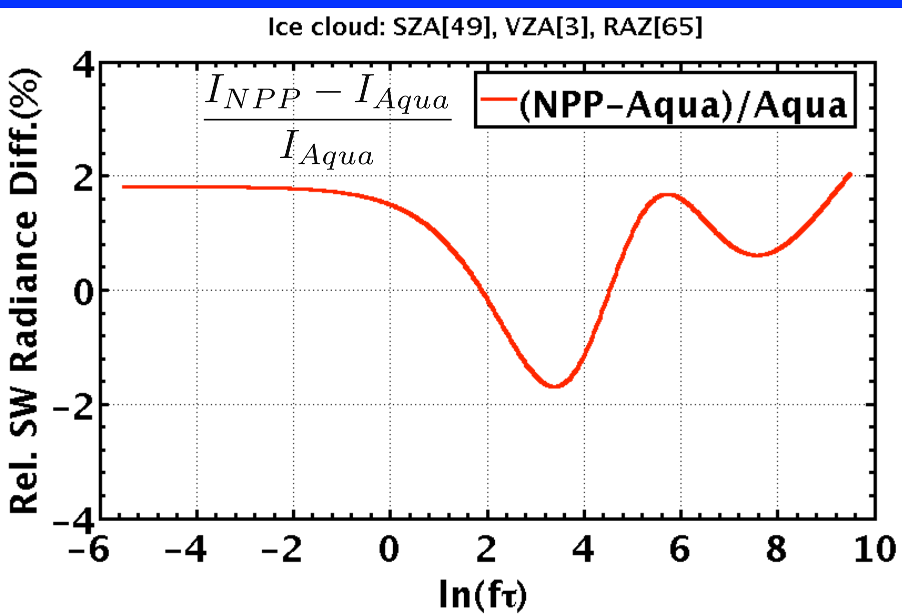

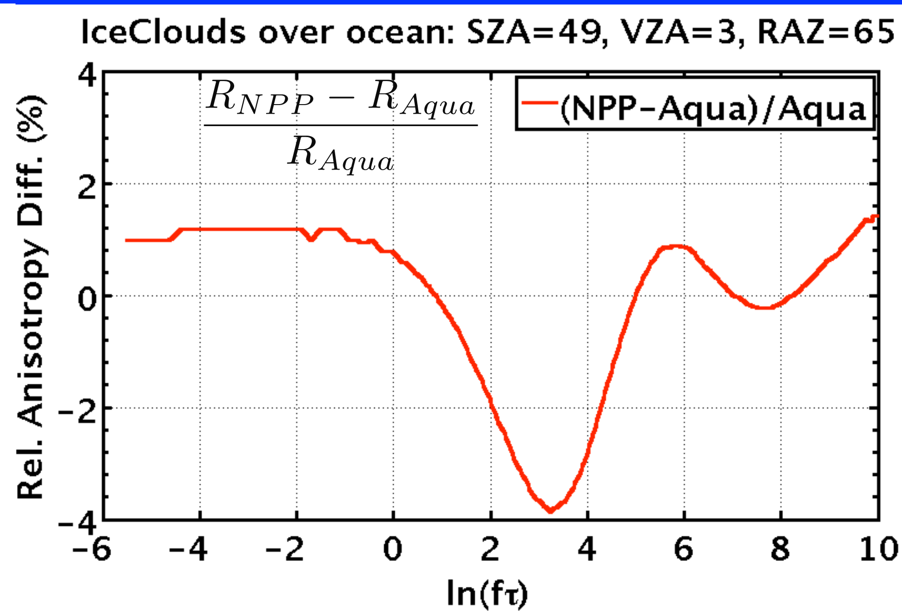

Simulate Aqua and NPP footprints to quantify flux error due to different footprint sizes

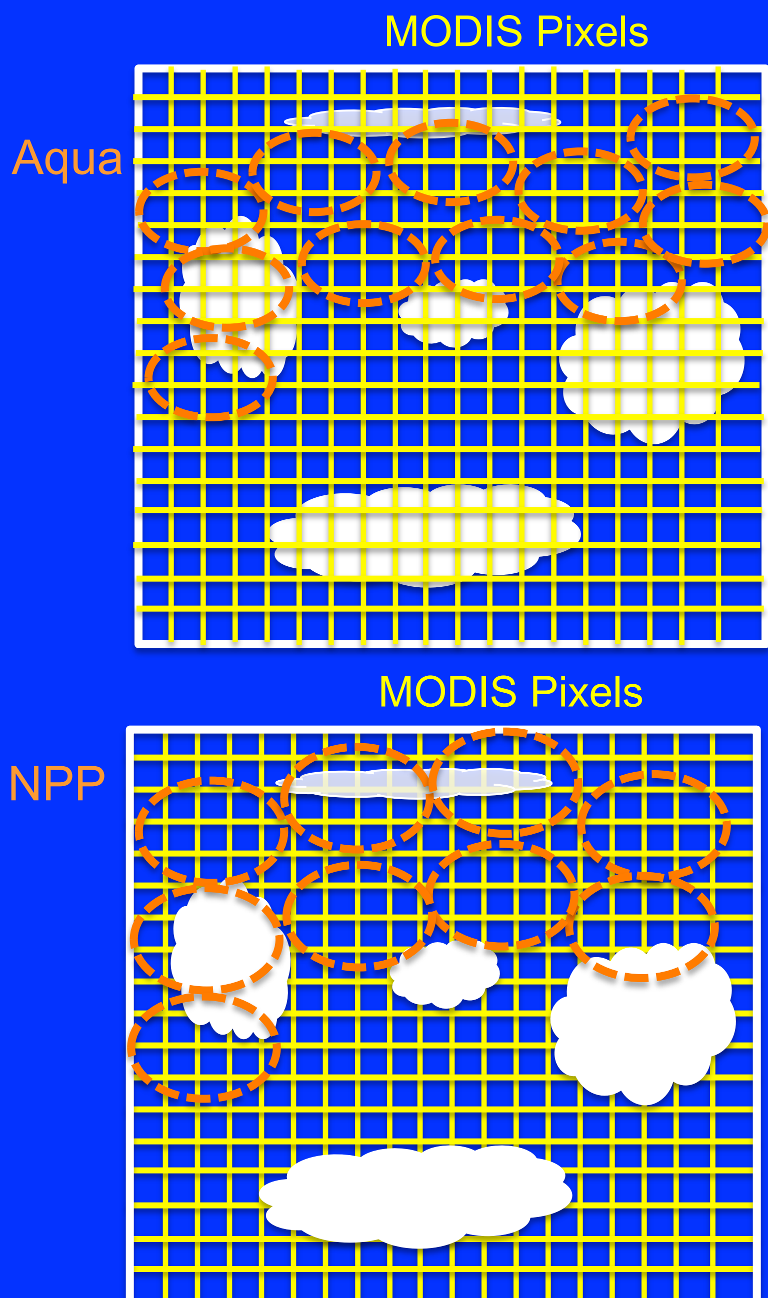

- Derive broadband radiances for these simulated Aqua and NPP footprints using MODIS spectral channels:

$$I_{sw}^{md} = d_0 + \sum_{j=1}^{7} d_j I_j$$

$$I_{lw}^{md} = a_0 + \sum_{j=1}^{5} a_j I_j$$

- Convert the broadband radiances to fluxes using Aqua ADMs and scene identification from MODIS

Develop narrowband-to-broadband (NB2BB) coefficients

- Use Aqua data from July 2002 to September 2007
- Shortwave
  - Use 7 MODIS spectral bands (0.47, 0.65, 0.86, 1.24, 2.13 and 3.7 µm) in the regression
  - Derive monthly coefficients for discrete intervals of solar zenith angle, viewing zenith angle, relative azimuth angle, surface type, snow/non-snow, cloud fraction, cloud optical depth
- Longwave
  - Use 5 MODIS spectral bands (6.7, 8.5, 11.0, 12.1 and 14.2 µm)
  - Derive monthly coefficients for discrete intervals of viewing zenith angle, precipitable water, surface type, snow/non-snow, cloud fraction, cloud optical depth

SW radiance from nb2bb agrees well with the CERES radiance

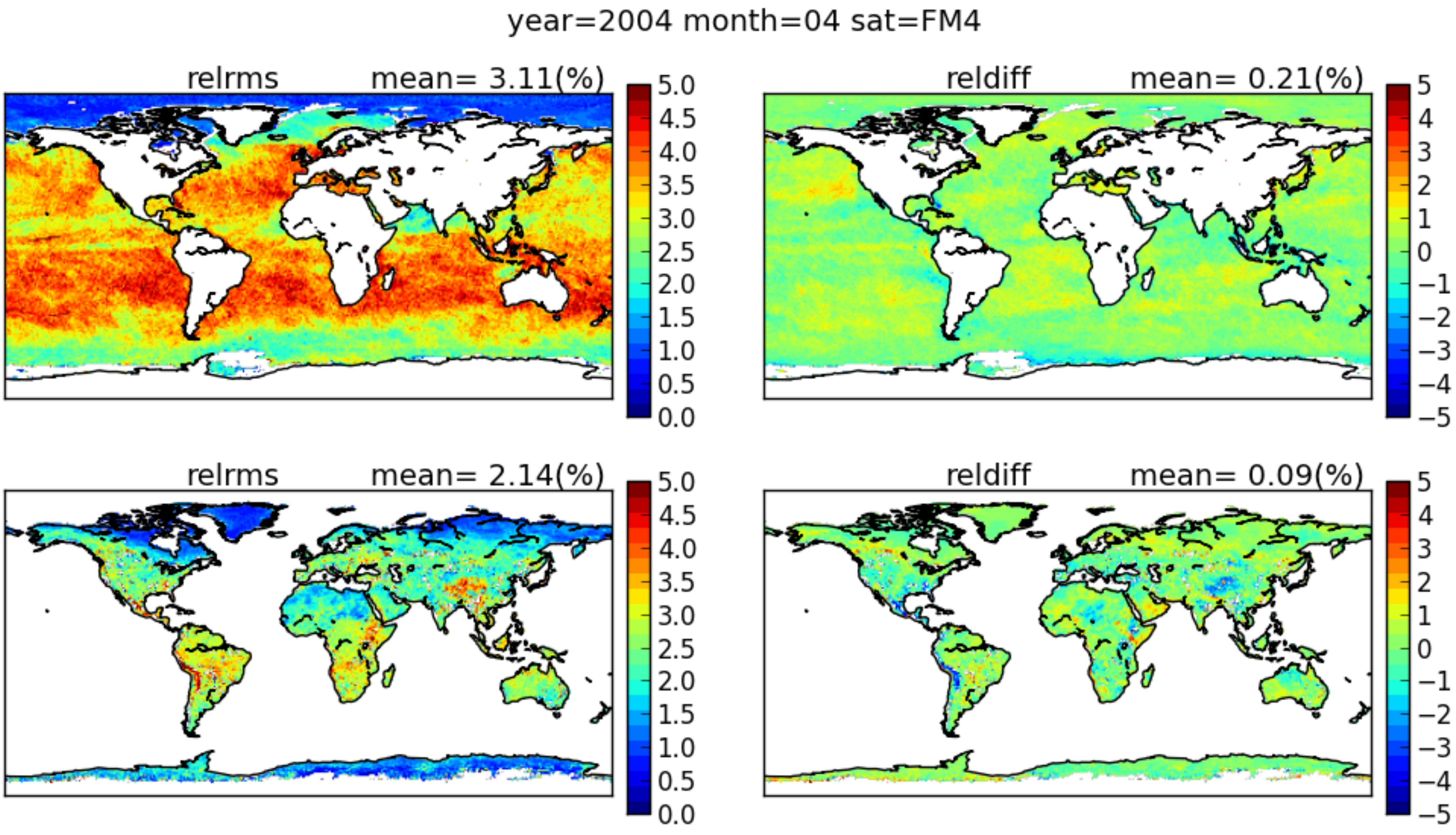

$$\sqrt{\frac{\sum\left(\frac{I_{nb2bb}-I_{ceres}}{I_{ceres}}\right)^2}{N}} \times 100\%$$

$$\sum \frac{(I_{nb2bb} - I_{ceres})}{I_{ceres}} \times 100\%$$

LW radiance from nb2bb agrees well with the CERES radiance

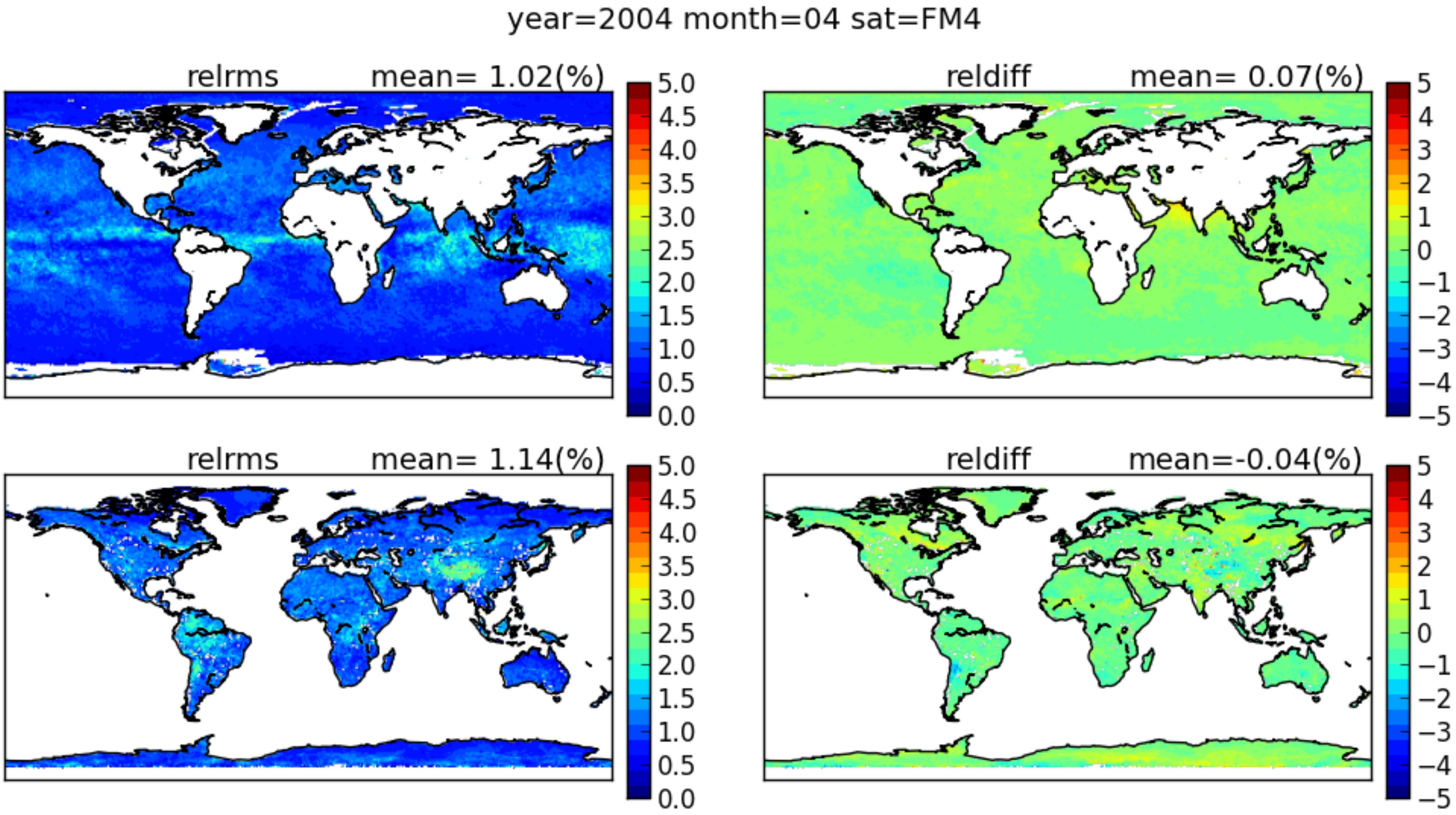

SW flux inverted from NB2BB radiance for Aqua footprint

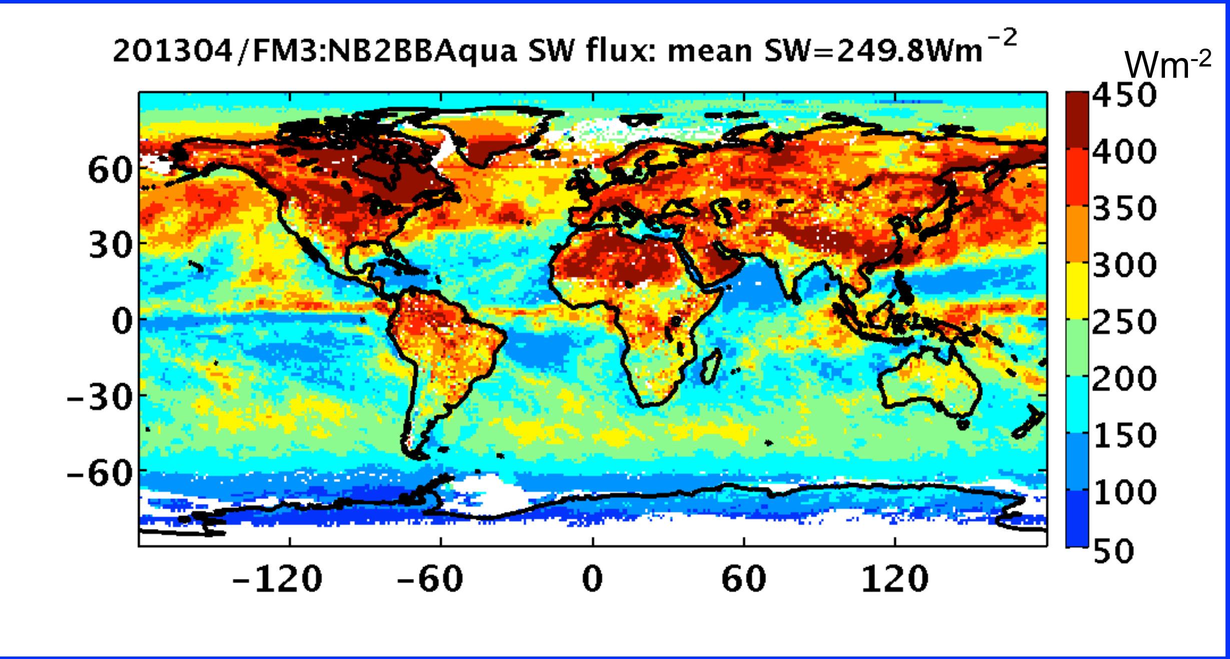

SW flux inverted from NB2BB radiance for NPP footprint

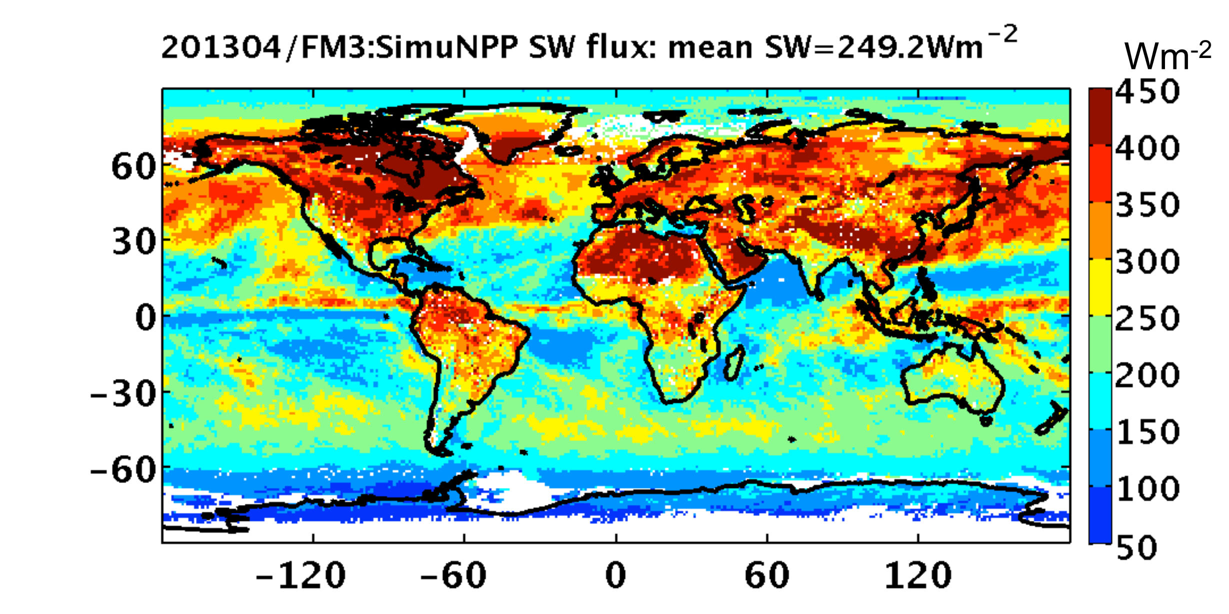

Global instantaneous monthly mean SW flux differs by 0.6 Wm^{-2} (0.25%)

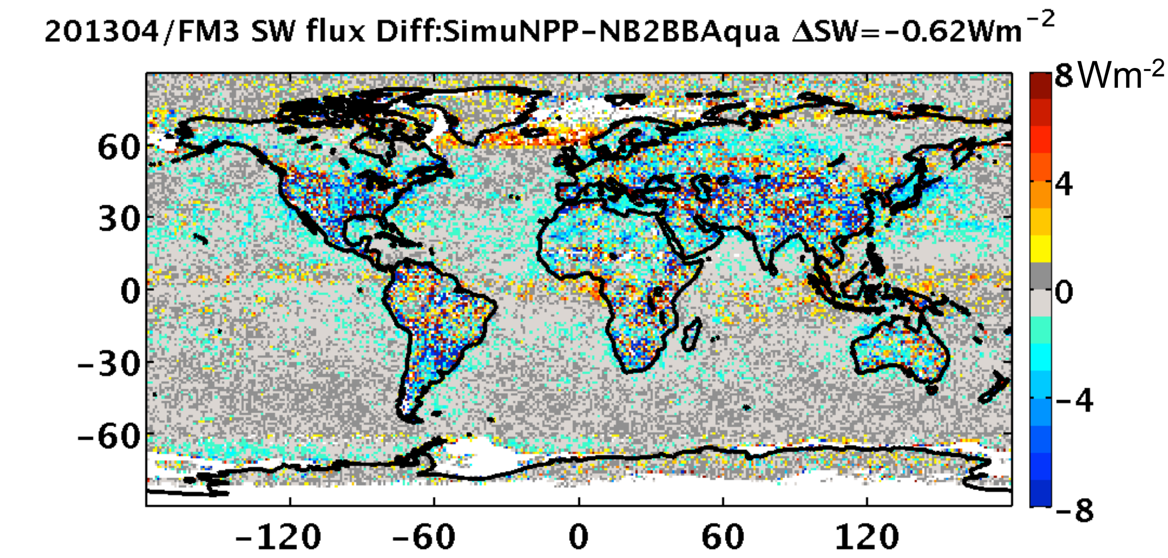

~81% of grid boxes with flux differences less than 2 Wm-2

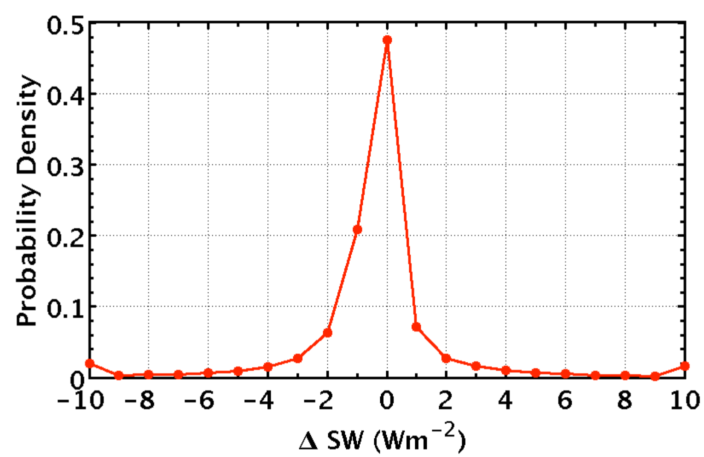

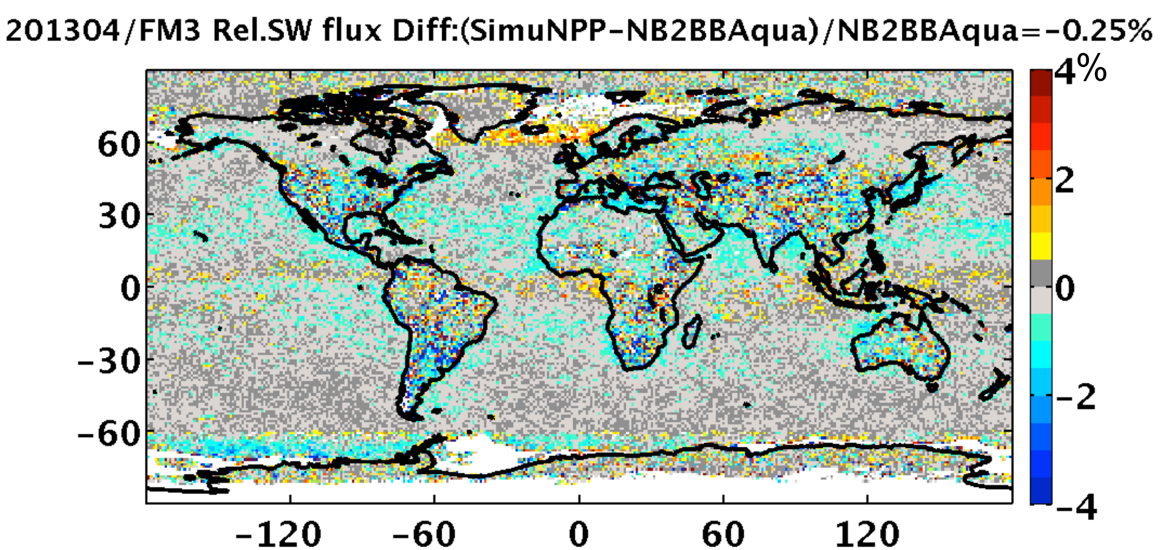

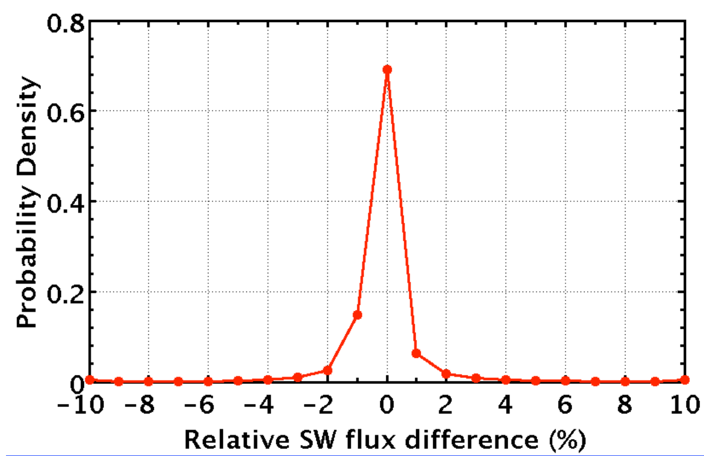

LW flux inverted from NB2BB radiance for Aqua footprint

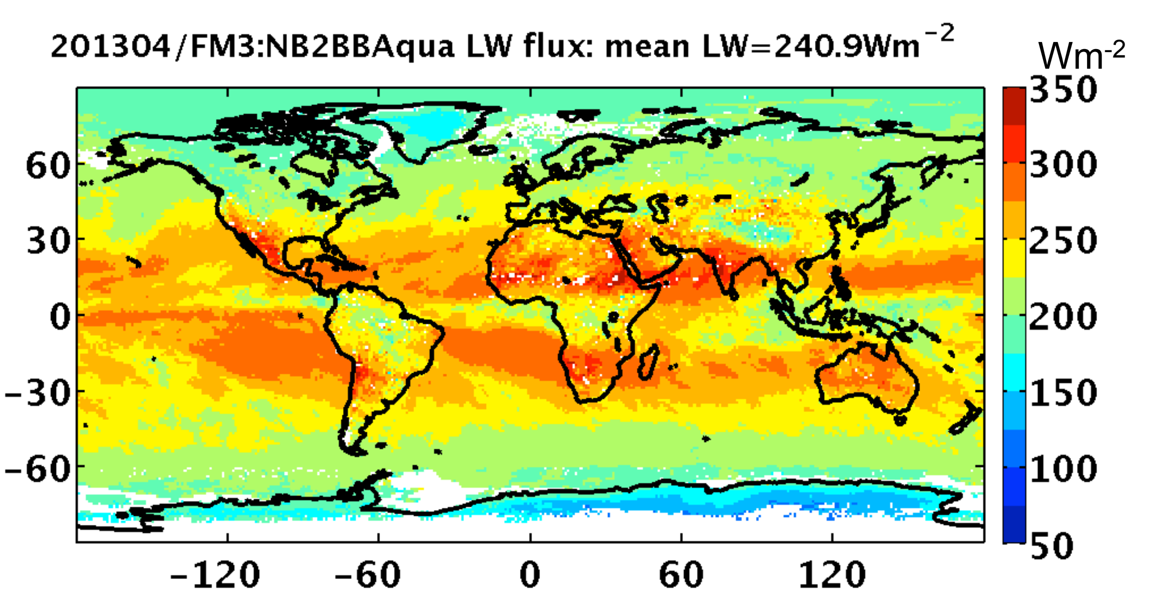

LW flux inverted from NB2BB radiance for NPP footprint

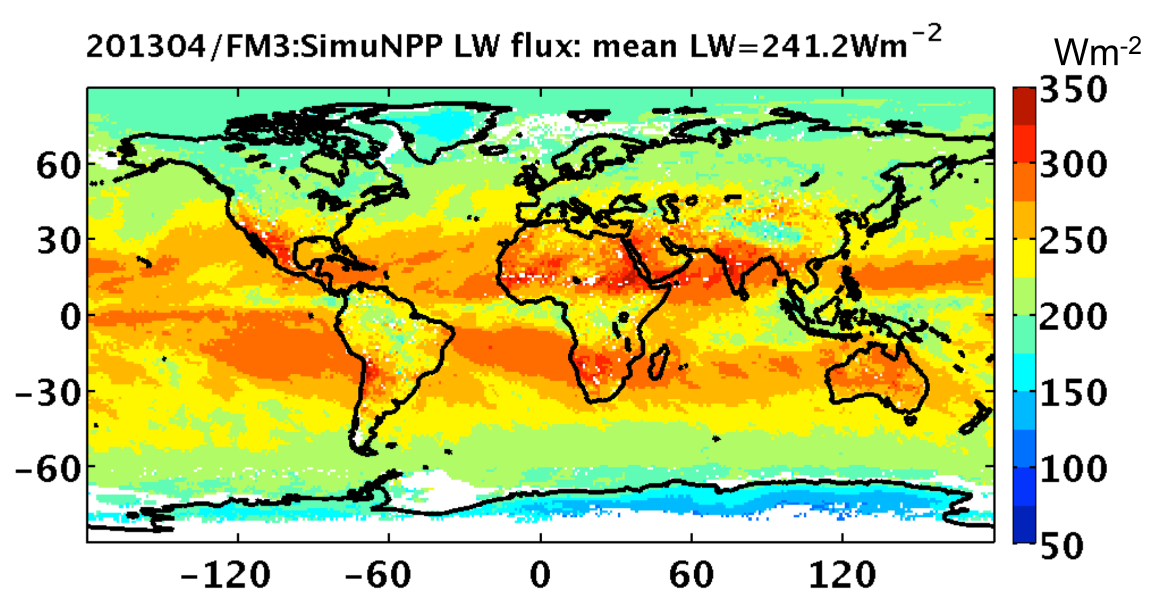

Global monthly mean daytime LW flux differs by 0.2 Wm^{-2} (0.1%)

201304/FM3 LW flux Diff:SimuNPP-NB2BBAqua $\Delta LW=0.22Wm^{-2}$

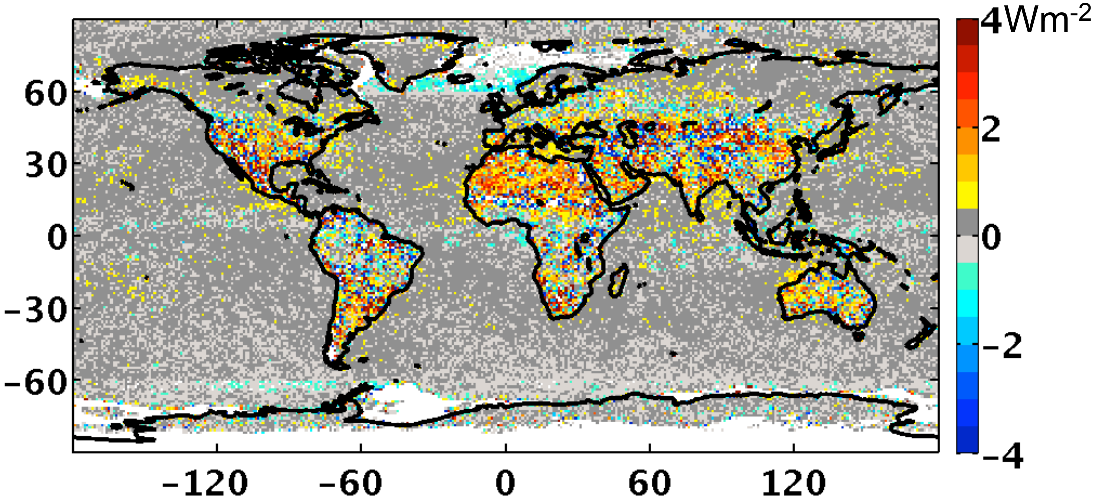

~94% of grid boxes with flux differences less than 2 Wm-2

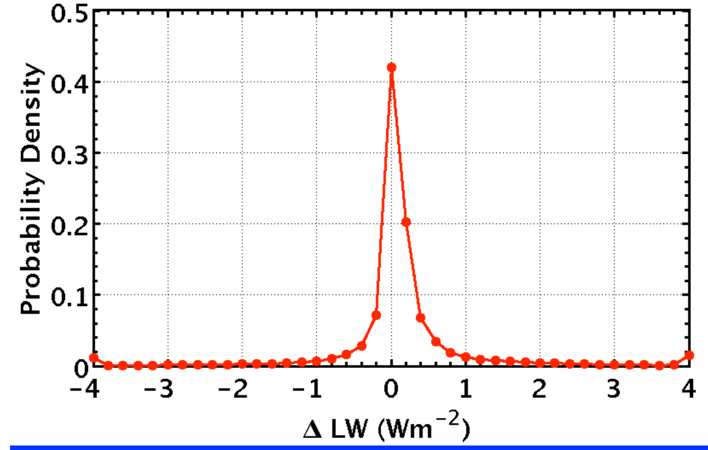

201304/FM3Rel. LW flux Diff:(SimuNPP-NB2BBAqua)/SimuNPP=0.09%

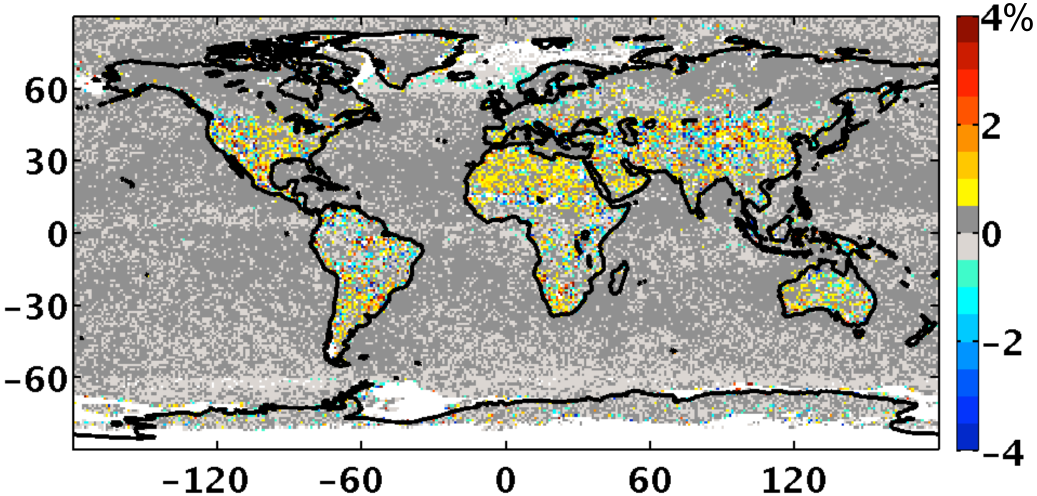

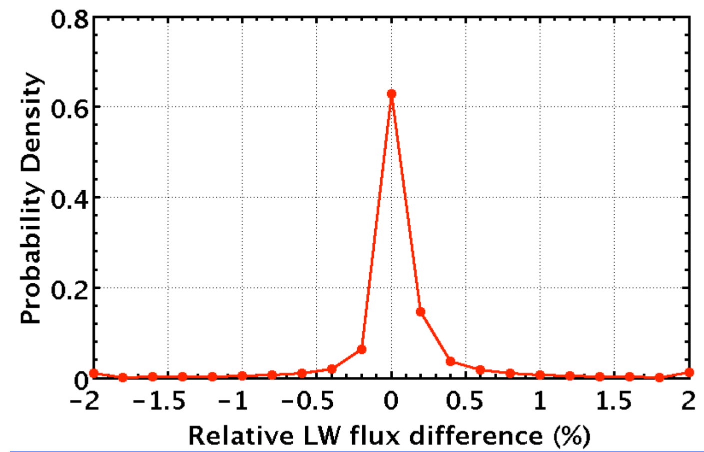

Global monthly mean nighttime LW flux differs by 0.2 Wm^{-2} (0.1%)

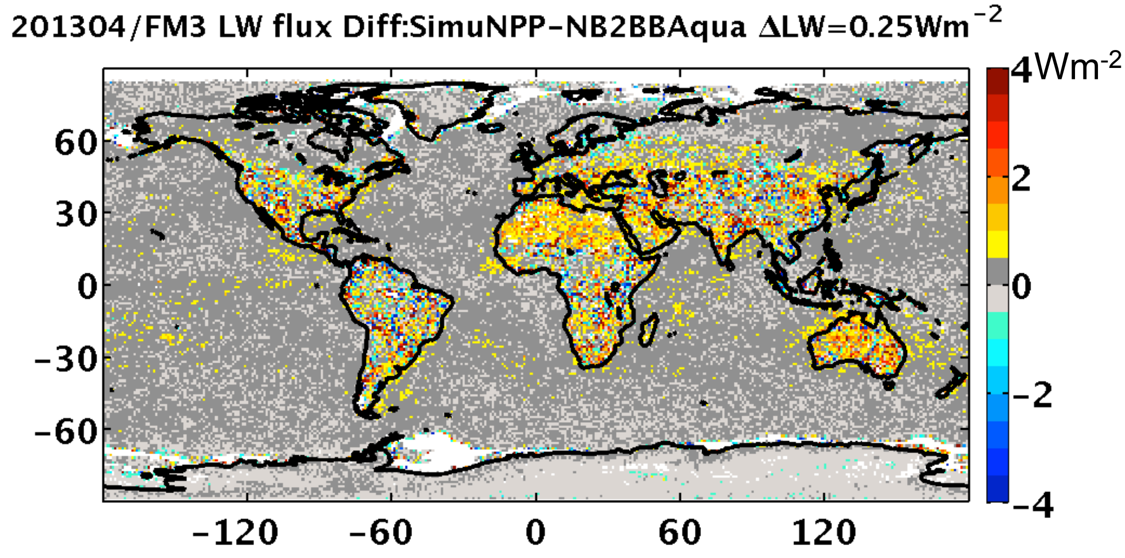

~96% of grid boxes with flux differences less than 2 Wm-2

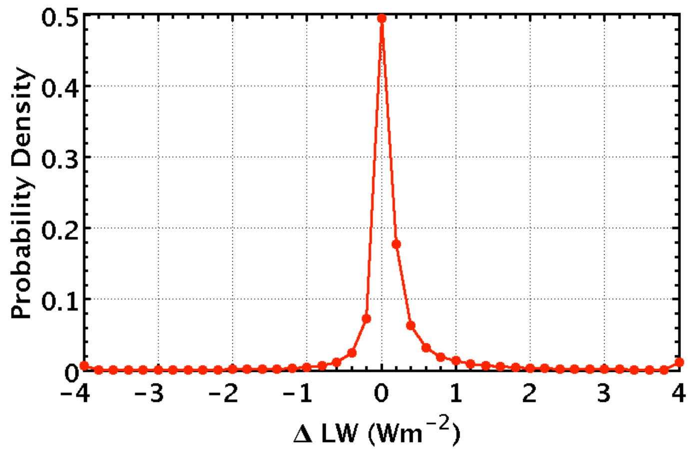

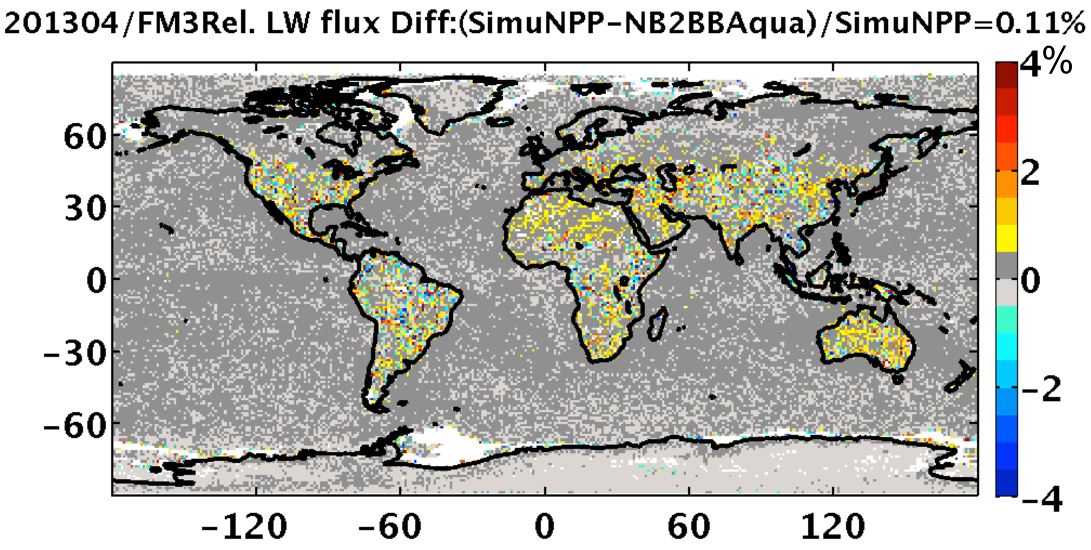

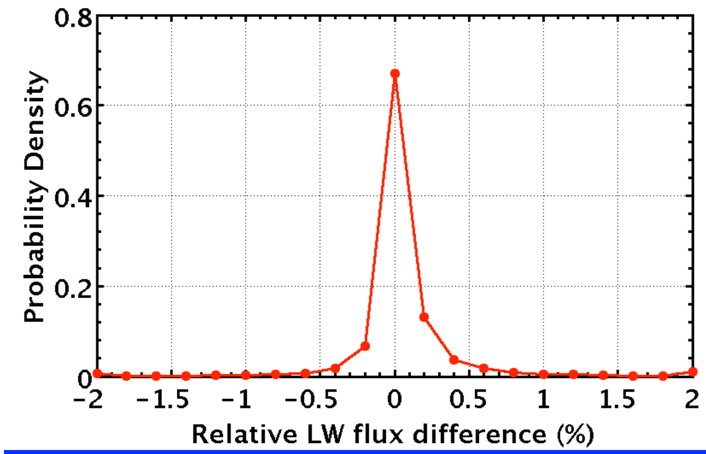

Does MISR radiance anisotropy change as footprint size changes ?

- SSFM data provide radiance anisotropy for each CERES along-track footprint from nine spatially matched directions
- CERES footprint size changes as viewing zenith angle changes
  - At nadir: 16 by 32 km
  - At θ=31°: 18.5 by 37 km
- Examine MISR 0.56 µm radiance anisotropy from these two different size of footprints:

$$I_{Aqua} = I(\theta_{CERES} < 20^{\circ})$$

$$I_{NPP} = I(30^{\circ} < \theta_{CERES} < 35^{\circ})$$

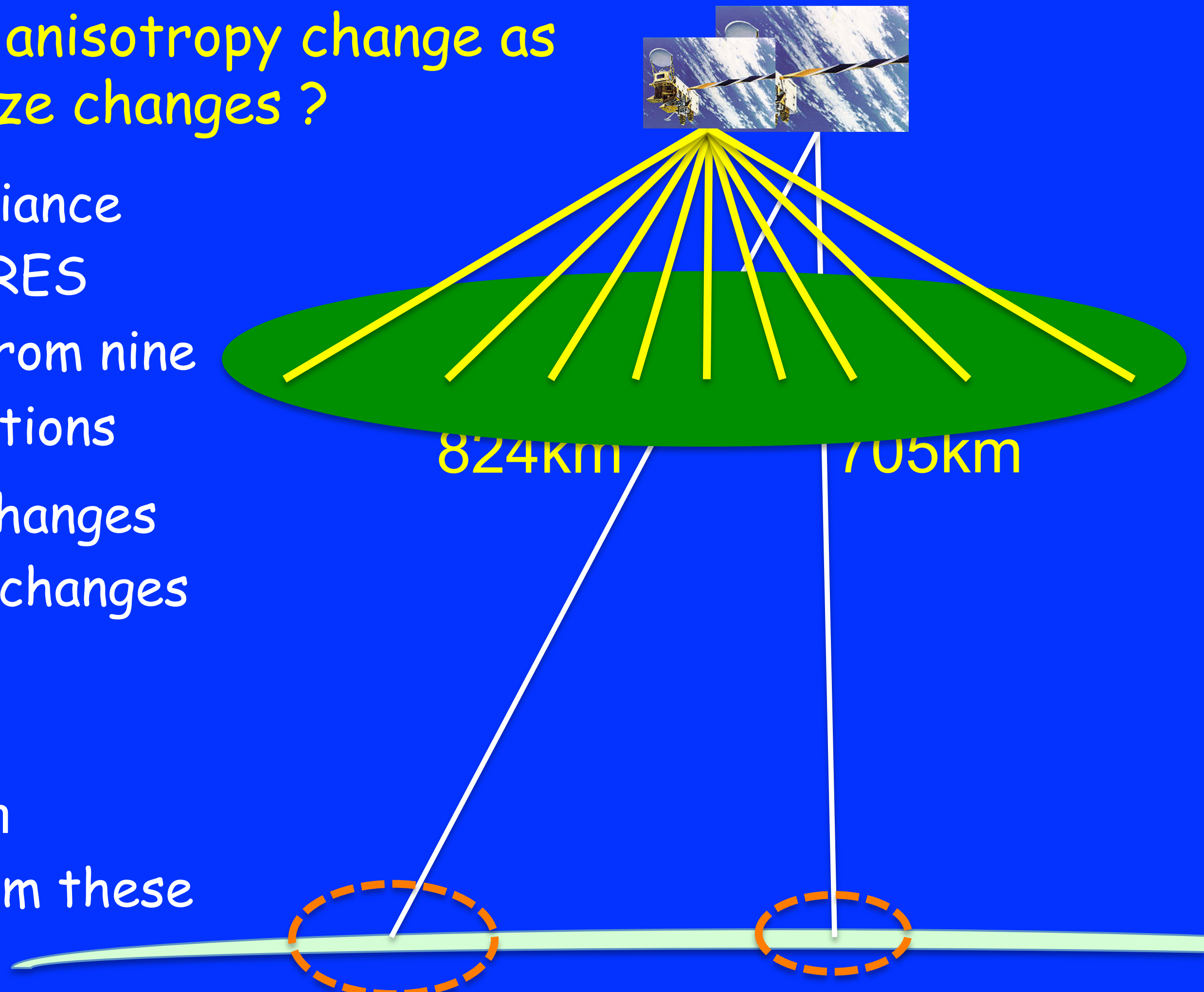

Radiance anisotropy from MISR for near-nadir-viewing CERES footprints

- Separate the near-nadir-viewing CERES footprints by solar zenith angle and relative azimuth angle
- Calculate the mean radiance for each camera angle for different cloud types
- Derive the "line-integrated" flux and anisotropy

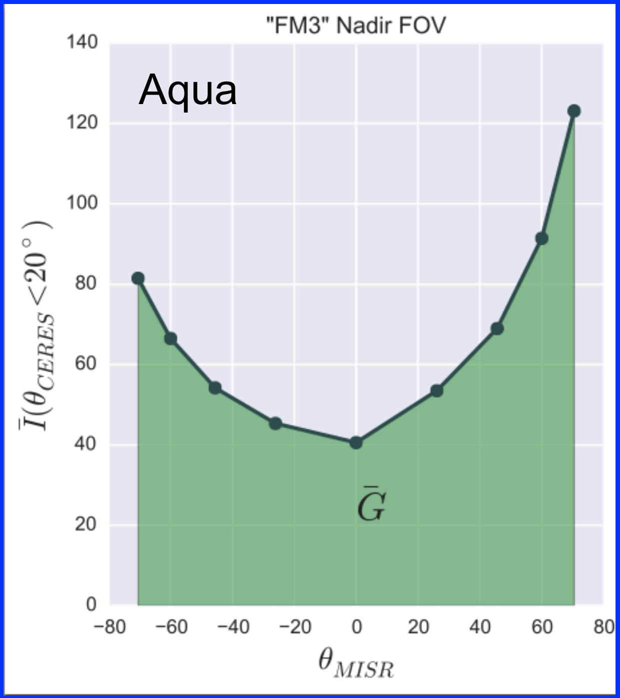

$$\bar{G} = \int_{-70.5}^{70.5} \bar{I}(\theta_{CERES} < 20^\circ) sin\theta cos\theta d\theta$$

$$R_{Aqua} = \frac{\pi \bar{I}(\theta_{CERES} < 20^\circ)}{\bar{G}}$$

PCL: CF =0.1-40%	High: EP<440 hPa	Thin: τ < 3.35
MCL: CF=40-99%	Mid: EP = 440-680 hPa	Mod: τ = 3.35 -22.63
OVC: CF=99-100%	Low: EP > 680 hPa	Thick: τ > 22.63

Derive flux from the MISR radiance measurement for oblique-viewing CERES footprints

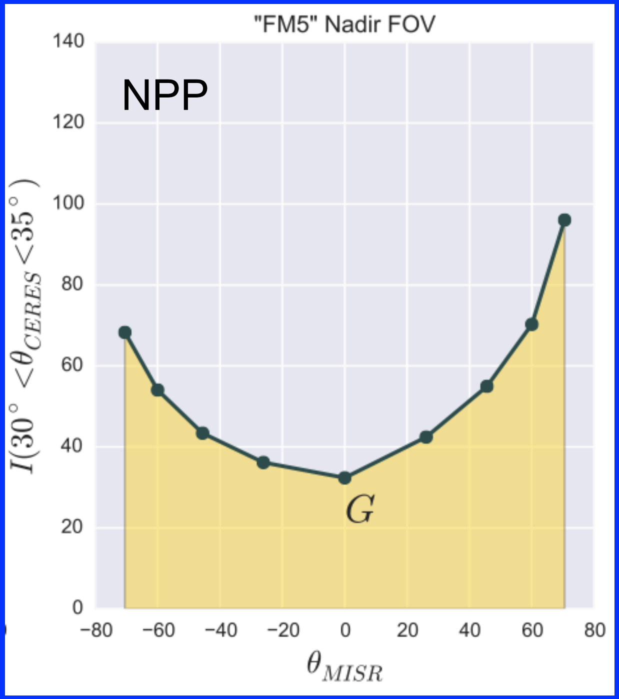

$$G = \int_{-70.5}^{70.5} I(30^\circ < \theta_{CERES} < 35^\circ) sin\theta cos\theta d\theta$$

$$R_{NPP} = \frac{\pi I(30^\circ < \theta_{CERES} < 35^\circ)}{G}$$

$$G_{ADM} = \frac{\pi I(30^\circ < \theta_{CERES} < 35^\circ)}{R_{Aqua}}$$

$$\frac{R_{NPP} - R_{Aqua}}{R_{Aqua}} \qquad \frac{G - G_{ADM}}{G_{ADM}}$$

Relative anisotropy and flux differences for low clouds

Partly cloudy: CF =0.1-40%
Mostly cloudy: CF=40-99%
Overcast: CF=99-100%
High: EP<440 hPa
Mid: EP = 440-680 hPa
Low: EP > 680 hPa
Thin: τ < 3.35
Mod: τ = 3.35 -22.63
Thick: τ > 22.63

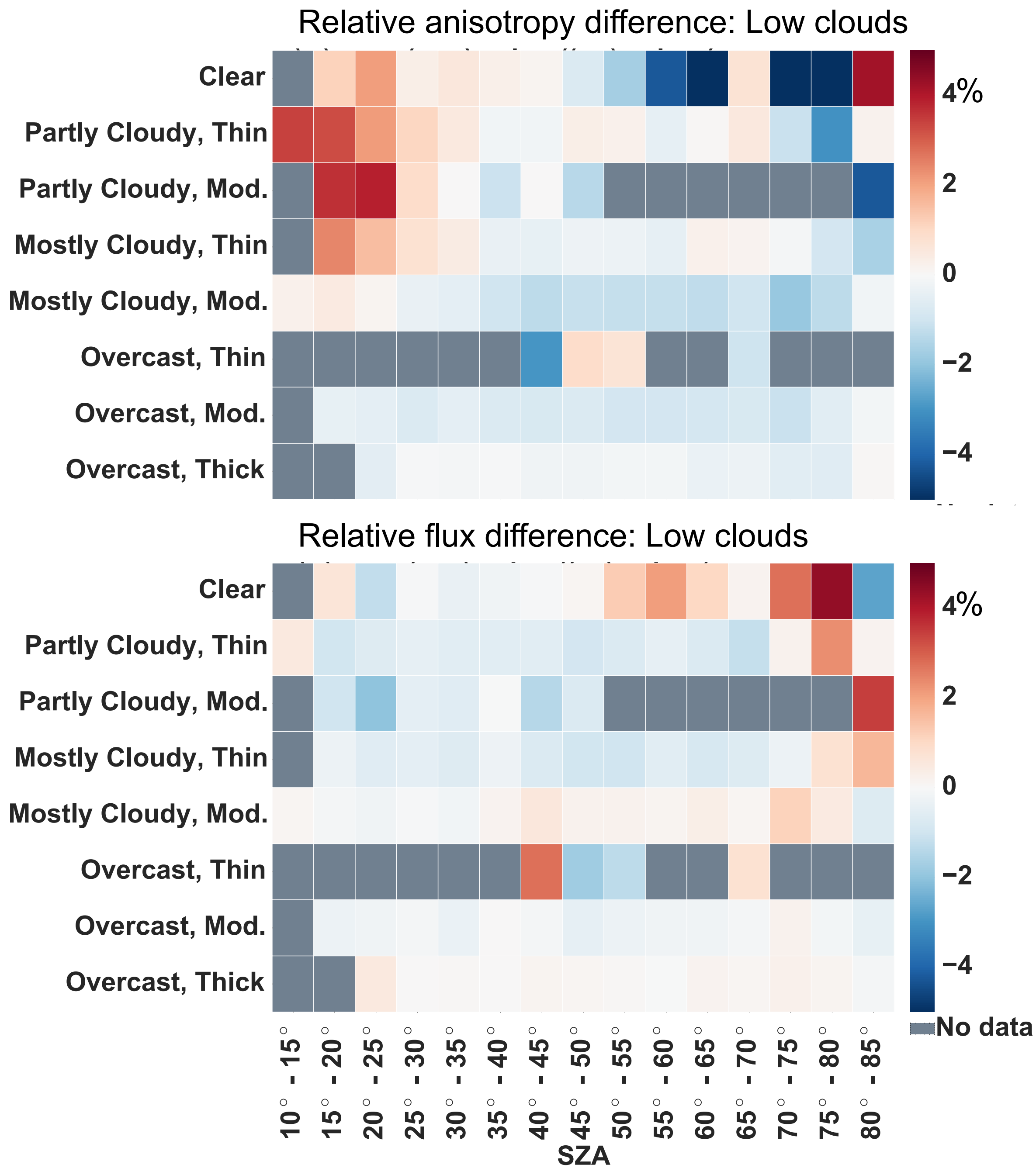

The relative flux difference ranges from 1.3% (75°<SZA<80°) to 0.1% (40°<SZA<45°).

Relative anisotropy and flux differences for mid clouds

Partly cloudy: CF =0.1-40%
Mostly cloudy: CF=40-99%
Overcast: CF=99-100%
High: EP<440 hPa
Mid: EP = 440-680 hPa
Low: EP > 680 hPa
Thin: τ < 3.35
Mod: τ = 3.35 -22.63
Thick: τ > 22.63

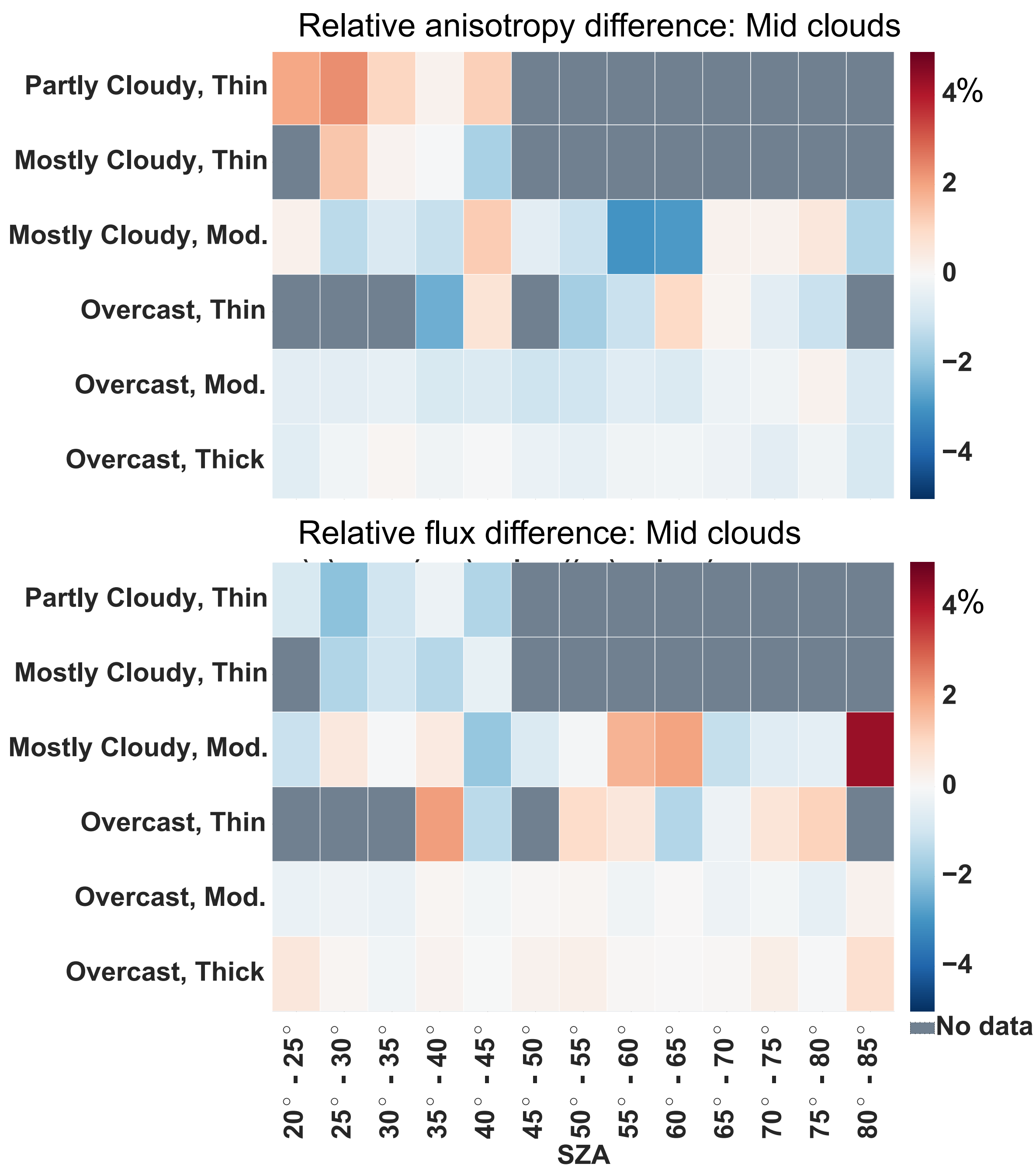

The relative flux difference ranges from 1.8% (80°<SZA<85°) to 0.0% (70°<SZA<75°).

Relative anisotropy and flux differences for high clouds

Partly cloudy: CF =0.1-40%
Mostly cloudy: CF=40-99%
Overcast: CF=99-100%
High: EP<440 hPa
Mid: EP = 440-680 hPa
Low: EP > 680 hPa
Thin: τ < 3.35
Mod: τ = 3.35 -22.63
Thick: τ > 22.63

The relative flux difference ranges from -0.7% (50°<SZA<55°) to -0.1% (35°<SZA<40°).

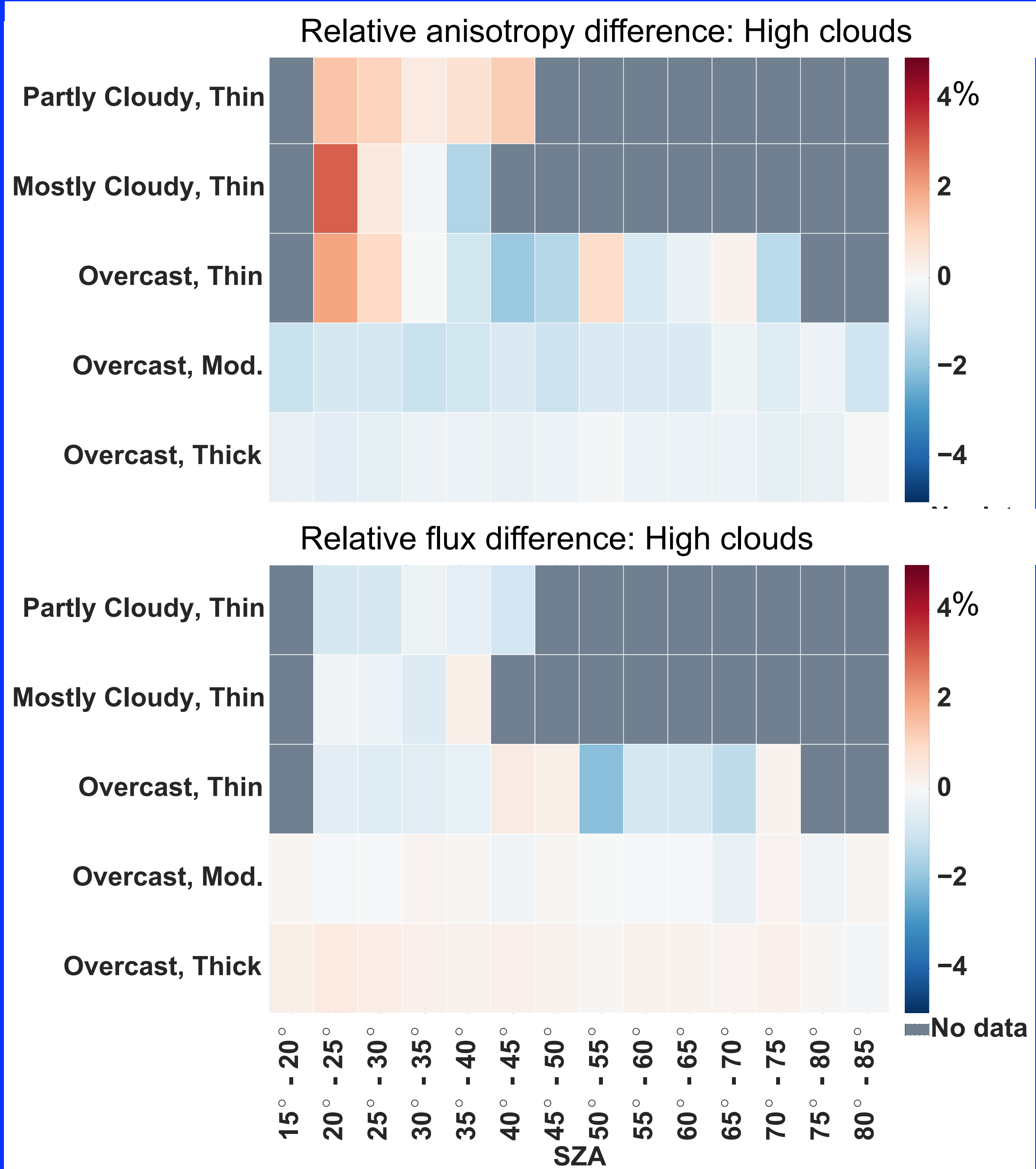

Summary

- Compared the radiance vs. ln(fτ) relationship derived using CERES-Aqua with that derived using CERES-NPP
  - Anisotropy factors over cloudy ocean can differ by up to 4% for thin partly cloudy scenes
- Generated a month of simulated NPP observations using Aqua-MODIS
  - MODIS spectral radiances in the simulate NPP footprints and Aqua footprints are converted to broadband radiances
  - Fluxes are derived using these broadband radiances and Aqua ADMs
  - Global monthly mean instantaneous SW flux differ by 0.6 Wm^{-2} (0.25%)
  - Global monthly mean instantaneous LW flux differ by 0.2 Wm^{-2} (0.1%)
- MISR multi-angle measurements indicated that
  - The 'line-integrated' anisotropy can differ by up to 4% for thin partly cloudy cases, and by less than 1% for moderate and thick overcast cases
  - The overall relative flux biases are less than 0.5% for different solar zenith angles